Pergamon

Journal of Vestibular Research, Vol. 5, No. 6, pp. 421–442, 1995

0957-4271/95 $9.50 + .00

0957-4271(95)00021-6

Original Contribution

WHEN PUSH COMES TO SHOVE: COMPENSATION FOR PASSIVE PERTURBATIONS OF THE HEAD DURING NATURAL GAZE SHIFTS

Julie Epelboim,[1] Eileen Kowler,[2] Robert M. Steinman,[1] Han Collewijn,[3] Casper J. Erkelens,[4] and Zygmunt Pizlo[5]

[1]Department of Psychology, University of Maryland, College Park, Maryland USA;
[2]Department of Psychology, Rutgers University, New Brunswick, New Jersey USA;
[3]Department of Physiology I, Erasmus University, Rotterdam, The Netherlands;
[4]Department of Biophysics, University of Utrecht, Utrecht, The Netherlands;
[5]Department of Psychological Science, Purdue University, West Lafayette, Indiana USA
Reprint address: Julie Epelboim, Department of Psychology, University of Maryland, College Park, MD 20742-4111 USA

☐ **Abstract – The effects of passive displacements to the head delivered by an abrupt push to the upper body were studied in human subjects during gaze shifts to nearby targets while the head was completely unrestrained. Accurate measurements of gaze were obtained via the Maryland Revolving Field Monitor, used to measure head and eye rotations unconfounded with translations, and by an acoustic ranging system, used to measure head translations. Compensation for head perturbations was quite good, with gaze errors much the same as gaze errors in the absence of the push. Compensation along one or both meridians was achieved by means of the vestibulo-ocular response in many of the gaze shifts. The results suggest an impressive ability to coordinate head and eye movements during natural gaze shifts, carried out by one or more different kinds of compensatory systems that the subject can access at will or according to task demands.**

☐ **Keywords – gaze shifts; vestibulo-ocular response; head movements; eye movements.**

Introduction

The properties of gaze shifts change when laboratory testing conditions are made more like those typically encountered in the natural world. For example, peak gaze velocity is faster during gaze shifts made while the head is free to move than when the head is stabilized by a biteboard (1,2). This finding was shown to be the result of a genuine enhancement of gaze produced by allowing motions of the head, and not the result of the addition of the velocity of the eye in the head to the velocity of the head in space. The enhancement is consistent with the idea that the natural tendency of the oculomotor system is to program head and eye movements jointly (3,4). Subsequent work showed that enhancement of gaze velocity, obtained when head movements were allowed, could be increased even further by requiring the subject to do a natural task (tapping a sequence of targets), rather than the artificial task of simply looking at the sequence of targets with no other goal or purpose in mind (5).

This paper continues the attempt to study oculomotor performance under more natural testing conditions than those typically employed in laboratory studies. In this study, we examined the effects of passive displacements of the head delivered while a gaze shift was in progress. Effects of passive displacements have been studied before (6–9). In these prior studies, however, the head was restrained to some degree either by helmets mounted so as to restrict head motion to horizontal rotations

Received 3 January 1995; Accepted 5 May 1995.

or by biteboards. In the present study, no head restraints were used, so both head and body were free to move in 3 dimensions in any way the subject chose during the gaze shift.

Our interest in the effects of passive displacements was inspired by recent observations showing that gaze shifts made between targets located near the subject can be extremely accurate (1,2). Accurate shifts of gaze between distant targets have been observed previously (see, for example, 3,6,7), but nearby targets present a special problem. When targets are nearby, translations of the head, as well as rotations, affect the position of the retinal image, with the effect of translations increasing the closer the target is to the eye. As a result, an accurate shift of gaze requires coordinating eye rotations with both head rotations and head translations, taking the effects of the distance between eye and target into account as well. Previous demonstrations that passive displacements delivered to the head do not impair the accuracy of gaze shifts between distant targets (6–9) attested to the presence of some mechanism that adjusted the rotation of the eye in the head to compensate for the passive head rotation. It is not known whether a comparable level of compensation would be available when targets are nearby and head translations must be taken into account as well. The study of gaze shifts with nearby targets (that is, within arm's reach) is quite important because such gaze shifts are critical for the performance of most natural visual-motor tasks (from chipping flint tools to sewing to surgery) and represent one of the most important contributions of eye movements to successful visual performance. It is for this reason that we developed the specialized instrumentation necessary to determine accurately the direction of gaze with respect to nearby, 3-D targets (details described in Methods).

The primary goal of this study was to find out whether the high level of compensation for passive displacements, demonstrated previously for distant targets and partially restrained heads, would also obtain: (1) under more natural testing conditions, when the head was allowed complete freedom of movement, and (2) when targets were near enough that translations of the head would have to be taken into account. Our second goal, should a high level of compensation be observed, was to investigate the source of this compensation. The previous studies (6–9) had identified two possible sources for compensation of passive displacements. One was the vestibulo-ocular response (VOR). The second was a gaze-control system that computed gaze position throughout the gaze shift and terminated the gaze shift when the intended goal position was reached. These two sources of compensation for passive displacements contribute to different degrees, depending on the subject, the task, or the size of the gaze shift (7–10).

We found high levels of compensation for passive displacements during natural gaze shifts performed between nearby targets. We also found evidence that both sources of compensation, the VOR and the gaze-control system described above, were operating during the course of gaze shifts, with the relative contribution of each varying from trial to trial.

Method

In this experiment we delivered natural passive displacements to a freely moving subject, who was looking from one target to another with no mechanical constraints on movements of his head or body. The subject shifted gaze between targets while, on a small proportion of the gaze shifts, an experimenter unexpectedly displaced the subject's head by abruptly pushing on the subject's upper back and shoulder. Details of the subjects, stimulus, procedure, recording instrumentation, and data analysis follow.

Subjects

Two of the authors served as subjects (CE and ZP). Both had extensive previous experience as eye movement subjects, including experiments in which free-headed gaze shifts were studied (1,2,11). CE and ZP were tested because each had some training in music (as did the experimenter, HC), and we felt this would be important in helping them use the metronome to control the timing of gaze shifts and

pushes, and thus increase the likelihood that pushes and gaze shifts would coincide appropriately. CE was tested in three and ZP in two 100-trial recording sessions. Testing was done under the conditions approved by the University of Maryland Human Subjects Committee.

Stimulus

The subject's task was to shift gaze between 3 widely spaced targets arranged in a triangular configuration. The arrangement of the 3 targets is shown in Figure 1a. The target at the apex of the triangle, farthest from the subject, is called the Center target. The targets at the base of the triangle were called Left and Right, respectively.

The targets were rods topped with 0.5-cm diameter colored LEDs placed into wells on a Worktable located in front of the subject. The distance between the subject's eye and the targets was on average about 50 cm, but since the head was totally unconstrained, this distance varied somewhat depending on momentary head position. The average angular

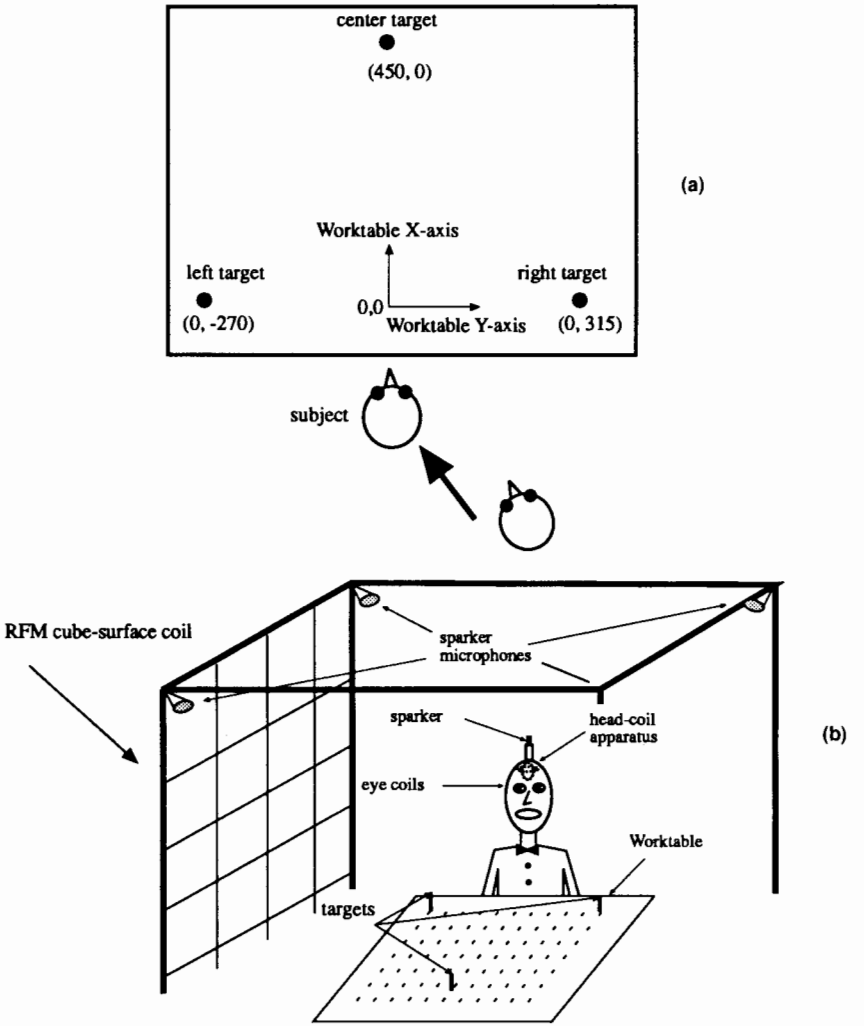

Figure 1. (a) Experimental setup for the push experiments showing the locations of the 3 targets. The numbers in parentheses show Worktable coordinates of each target in mm. (b) Schematic diagram of the Maryland Revolving-Field monitor.

separation between the Center target and either the Left or the Right target was 31° for subject CE and 37° for subject ZP. The average angular separation between the Left and Right targets was 50° for subject CE and 59° for subject ZP.

Targets were visible at all times. The experiments took place in a well-lit room in which background objects were present and visible.

Procedure

Each eye movement recording session contained 100 six-second trials and lasted about 30 minutes. At the start of the recording session, the experimenter turned on a metronome, which was set to beep every second.

Before each trial the subject began to shift gaze between the 3 targets, attempting to time each gaze shift so that it coincided with a beep from the metronome. The three targets were scanned either clockwise (Center-Right-Left) or counterclockwise (Center-Left-Right), with the scanning direction varied haphazardly by the subject from trial to trial. When the subject felt that a rhythmic scanning pattern had been established, he started the trial by means of a button push, initiating the collection of data.

One of the experimenters (HC) sat behind the subject and was responsible for delivering the passive displacements by pushing unexpectedly on the subject's shoulder and upper back. The experimenter wore gloves on each hand. Microswitches, mounted inside the palms of the glove, were sampled at 488 Hz and recorded the time that contact was made with the subject's body. The experimenter pushed the subject abruptly and infrequently, and in a variety of directions, in an attempt to discourage the subject from correctly anticipating the time of occurrence or the trajectory of the next push. The experimenter also used the metronome and attempted to control the timing of his pushes so that movements of the subject's head, resulting from a push, would be likely to coincide with the gaze shift. (As will be discussed below in the Data Analysis section, about 10% of the pushes met this criterion.) Among these trials, 82% contained a single push, 10% contained no pushes, and 8% contained two pushes.

Eye and Head Movement Recording

Apparatus. Eye and head movements were recorded using the Maryland Revolving Field Monitor apparatus (MRFM), sketched in Figure 1b. The details of the MRFM apparatus are described in references 11 and 12. Briefly, the MRFM consists of 3 subsystems:

1. The Revolving Field Monitor/sensor-coil subsystem (RFM) measures orientations of the eyes and the head. The RFM produces 3 mutually perpendicular, magnetic fields revolving at different frequencies. Each field is produced by two sets of ac-current-carrying, 5-element, coils mounted on a cubical frame—a "cube-surface coil" that produces a spatially homogeneous magnetic field within a large fraction of the frame's volume. Horizontal and vertical eye rotations are measured with silicone annulus-sensor coils (Skalar-Delft). Horizontal (yaw), vertical (pitch), and torsional (roll) head rotations are measured with the head-coil apparatus, consisting of 2 approximately perpendicular sensor-coils, mounted on the head. The angle between the plane of each eye or head sensor coil and the planes in which each magnetic field revolves is proportional to the difference between the phase of the ac-current induced in the sensor-coil and the phase of the ac-current induced in a reference coil associated with each field. This phase-detection method for recording eye movements was introduced by Collewijn (13). The precision of angle measurement in the RFM is better than 1 minarc with linearity better than 0.01%. Sampling rate was set to 488 Hz.
2. The Sparker Tracking Subsystem (STS) measures 3-D head translations. The "sparker," mounted on top of the head, emits bursts of sound at 61 Hz (sparker strobes) that are detected by 4 microphones mounted

on a rectangular frame near the ceiling. STS computes the time of arrival of each spark's wavefront and outputs distances to each microphone (to 0.1 mm).

3. The Worktable, which contains an 11 × 14 grid of equally-spaced wells into which targets can be placed, serves as the basis for a coordinate system into which all recorded quantities are converted (see Figure 1b).

The MRFM collected and stored data from its three subsystems in discrete "bursts," each containing 12 signals produced by the RFM, the STS, and the gloves worn by the experimenter. During each second, 488 RFM-bursts were obtained and stored. Only 1 in 8 RFM-bursts contained new sparker values because there were only 61 sparker strobes/s. Intermediate sparker values were linearly interpolated.

Analysis

Details of the analyses of the MRFM data are described in references 11 and 12. The main steps involved in converting raw data into useful quantities are summarized below.

Calibrations. Outputs of the RFM and the STS were converted into Worktable-coordinates to determine where the subject was looking with respect to the targets. To do this, three types of calibrations were performed: (1) A sparker placed in wells at different locations on the Worktable calibrated "sparker-space"; (2) Sighting centers of each eye were measured with the head in a reproducibly-known position on the biteboard, using a sighting technique; (3) The orientations of the eyes that corresponded with the line-of-sight pointing in a known direction (along the positive x-axis of the Worktable) were measured at the start of each recording session by having the subject look at each of his pupils reflected in a mirror, which was arranged to be parallel to the Worktable y-axis. During the same mirror-trials, positions of the sensor coils on the eyes, the position of the head-coil apparatus on the head, and the relationship of the sparker to the eye and head coils were also measured.

Line-of-sight vectors. The line-of-sight vector of an eye was defined as the vector from the sighting center of that eye, pointing in the direction of the eye's orientation, measured with the sensor coil. The positions of the subject's sighting centers with his head in a known biteboard position were measured before the recording sessions began. The orientations of the eyes that corresponded to the line-of-sight being aligned with the positive x-axis were measured during mirror-trials. Given this information and the reading of the head-coils, sparker, and eye coils, the subject's lines-of-sight at an arbitrary RFM-burst could be calculated.

Eye-in-head vectors. The orientation of the eyes relative to the head was calculated using Helmholtz coordinates (14). The First Helmholtz angle (H_1), corresponding to the eye's vertical angle (pitch or elevation) was defined as the rotation of the eye around the "baseline," where baseline was the line connecting the sighting centers of the two eyes. The Second Helmholtz angle (H_2), corresponding to the eye's horizontal angle (yaw or azimuth) was defined as the rotation of the eye around the vector that was parallel to the positive z-axes of the Worktable when the head was on the biteboard during the mirror trial. This vector is perpendicular to both the baseline and the line-of-sight vector when the subject looks straight ahead. The axes that define the Helmholtz coordinate system are fixed to the subject's head and move with it.

Instantaneous velocities. Gaze (eye-in-space) velocity at an arbitrary RFM-burst i was defined as the angle between the line-of-sight vector at burst i and the line-of-sight vector at burst $i + 1$. This quantity represents the eye's angular velocity in minarc/burst and can be converted to degrees per second by multiplying by 8.13 (488 bursts/s/60 minarc/°). This definition of velocity combined horizontal and vertical eye angles and was unsigned.

Eye-in-head velocity at an arbitrary RFM-burst was calculated in the same way as gaze velocity, except that eye-in-head vectors were used instead of the line-of-sight vectors.

For some analyses it was necessary to show horizontal and vertical eye-in-head velocities separately. In that case, the horizontal eye-in-head velocity at RFM-burst i was defined as the eye's second Helmholtz angle (H_2) at burst $i + 1$ minus H_2 at burst i, and the vertical eye-in-head velocity at burst i was defined as H_1 at burst $i + 1$ minus H_1 at burst i.

Horizontal and vertical head velocities in Helmholtz coordinates were defined as the angles the head rotated between bursts i and $i + 1$ around the vertical and horizontal Helmholtz axes as calculated at burst i.

Position of target with respect to the head. Target angles in eye-in-head (Helmholtz) coordinates were defined as the horizontal and vertical eye-in-head angles of the eye that would be measured if the subject were looking at that target. Target-angles move with the head as it rotates and translates, so fluctuations of the target angle represent changes in retinal target position as a result of the head movements.

Gaze-errors. Gaze errors were determined at the time of the offset of the first gaze shift made to the target. Secondary or corrective saccades, which occurred after most of the gaze shifts, were ignored. Gaze-error of each eye with respect to a target was defined as the angle between the line-of-sight vector at gaze shift offset and a vector from the eye's sighting center to that target.

Gaze shift detection. Gaze shifts were detected by exhaustive examination of all eye movement recordings by two observers, working independently. Recordings were displayed on the screen of a *SUN SparcWorkstation-GS*, and the observers marked approximate gaze shift onsets and offsets using a cursor controlled by a mouse. Gaze shifts occurring in the first or last 200 msec of a trial were excluded from further analysis. Each detected gaze shift was then classified according to whether it coincided with a push delivered by the experimenter (see Procedure section), where the occurrence of a push was determined from the output of the microswitches worn in the experimenter's gloves. Gaze shifts without pushes occurring either during the gaze shift or earlier in the same trial were classified as "control" gaze shifts. Gaze shifts occurring after a push was delivered in a trial were excluded from further analysis because the prior occurrence of a push in a trial may have affected gaze trajectory. The remaining gaze shifts, coinciding with pushes, were then examined to determine whether the passive displacement of the head produced by the push had coincided closely enough with the gaze shift to make examination of its effects meaningful. A strict criterion was used, namely, a gaze shift was designated as a "push gaze shift" when either horizontal or vertical head velocity exceeded the mean of the head velocity in control gaze shifts by one standard deviation by the time the saccade reached its peak velocity. Of the approximately 500 pushes delivered to the subject, 64 gaze shifts met this criterion and were classified as "push gaze shifts." All of these push gaze shifts took the head in the direction of the gaze shift because it was much easier and took less time to move the subject in the same direction as his body and head were already moving than in the opposite direction. Had this been noticed while the data was being collected, an attempt could have been made to modify the time and force of some of the pushes to produce push gaze shifts in both directions; a much harder push, delivered earlier with respect to the gaze-shift would have been required to displace the head opposite to its on-going motion. Future work on this problem would benefit by taking this problem into account.

Results

Trajectories of Head and Gaze During Gaze Shifts

To evaluate the effects of the pushes on gaze error we first examined the 2-dimensional trajectories of head and gaze during gaze shifts

superimposed on the surface of the Worktable. Gaze position on the Worktable was defined as the intersection of the line-of-sight vector and the plane parallel to the Worktable at the height of the targets (the target plane). Head position on the Worktable was defined as the intersection of the "head-vector" with the target plane. The head-vector was defined as the vector fixed to the head, with the origin at the midpoint of the baseline (the line connecting the sighting centers, see Methods). At gaze-shift onset, the direction of the head vector was set to coincide with the direction as the right eye's line-of-sight vector.

Figures 2 and 3 plot examples of head and gaze trajectories during the gaze shifts. The gray band shows the mean ±1 SD of the trajectories of the control gaze shifts. The dotted lines show trajectories of the individual gaze shifts containing pushes. Each plotted point was obtained from a single burst of the RFM, thus, the distance between the points increases with increasing gaze or head velocity.

Figures 2 and 3 show that control gaze shifts were accomplished in part by movements of the head, with the extent of the head movement varying depending on the subject and the intertarget distance. The control gaze shifts were, by and large, quite accurate, with the line of sight landing close to the position of the targets.

The wide scatter of the head trajectories during the push gaze shifts shows that the head was indeed deviated from its usual path by the push. Yet, remarkably, gaze deviated only modestly from its usual path and gaze landed on target. Thus, the eye must have been moving so as to compensate for the head perturbations because gaze shifts containing pushes appear very similar to control gaze shifts.

The following sections will provide quantitative support and amplification of these assertions.

Effects of the Pushes on Movements of the Head

In order to determine how much the head was affected by the push, we compared head angular velocity of push and control gaze shifts. Head velocity, calculated as the instantaneous angular velocity of the head vector during the RFM bursts when gaze velocity was at its peak, is shown in Figure 4 (lefthand graphs). Head velocity was 3 to 5 times higher during push gaze shifts (open triangles) than during control gaze shifts (filled circles). The difference was statistically reliable for both subjects ($t[879] = 9.9$, $P < 0.001$, for subject CE; $t[584] = 9.0$, $P < 0.001$, for ZP).

The effect of the push on head movements was also summarized by the distance the sparker (mounted on the head) moved during the gaze shift. Once again, as Figure 4 (righthand graphs) shows, the effect of the push was large and statistically reliable ($t[879] = 13.9$, $P < 0.001$, for CE; $t[584] = 7.8$, $P < 0.001$, for ZP). The movement of the head, if uncompensated, would have produced a large error in gaze. For example, a movement of the head of 50 mm should produce a gaze error about 5° greater than the gaze errors of control gaze shifts at the usual 50-cm distance between subject and target. Gaze errors, as summarized in the next section, were smaller than this.

The Effect of the Pushes on Gaze Errors

Gaze errors, measured at the offset of the gaze shift, are shown in Figure 5 for push and control gaze shifts and for the different gaze shift directions. (Right eye performance is shown. Left eye and binocular gaze errors were similar.) Gaze errors were only slightly larger for the push gaze shifts than for control gaze shifts, and the differences were not reliable. For CE, average gaze error was 2.7° (SD = 1.7, $N = 852$) for control gaze shifts and 3.4° (SD = 2.6, $N = 29$) for push gaze shifts. For ZP, average gaze error was 3.4° (SD = 1.5, $N = 551$) in control gaze shifts and 3.4° (SD = 1.6, $N = 35$) in push gaze shifts. Analysis of variance (gaze shift type: control or push × gaze shift direction) showed no significant main effect of gaze shift type (push compared to control) ($F[1, 869] = 2.9$, $P > 0.08$, for CE;

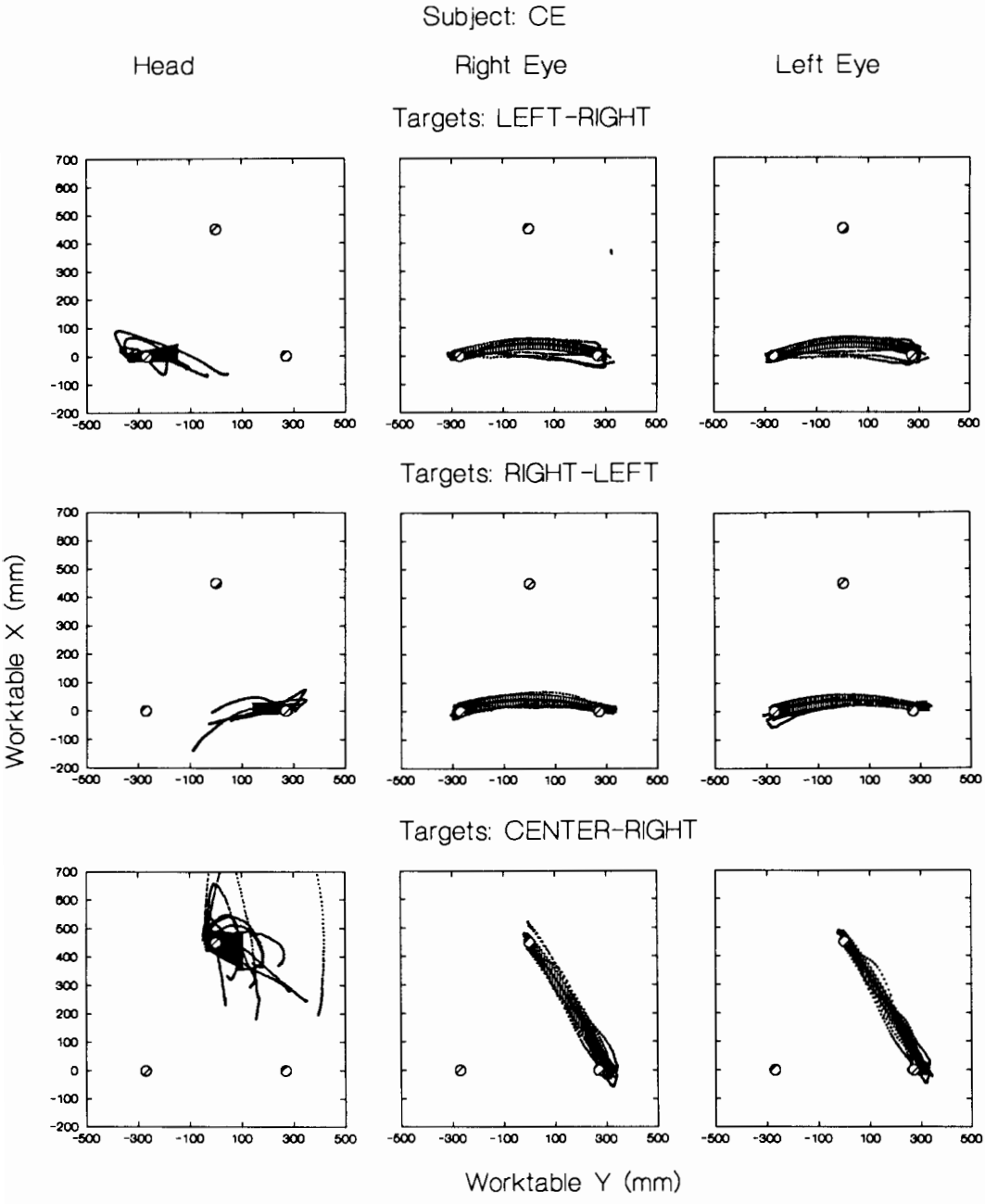

Figure 2. Subject CE: Two-dimensional trajectories of head (left) and gaze of the right (middle) and left (right) eye superimposed on the Worktable. Thick black bands are from control gaze shifts (mean ± 1 SD); individual thin traces are from push gaze shifts. Open circles denote target position.

$F[1, 574] = 0.02$, $P > 0.8$ for ZP). There was a significant interaction of gaze shift type and direction for CE ($F[5, 869] = 2.3$, $P < 0.001$), for whom the effect of perturbation was greater with the larger target separations (Left-Right or Right-Left) than with smaller target separations (see Figure 5), but not for ZP ($F[1, 574] = 1.1$, $P > 0.3$).

This analysis of gaze errors shows that pushes were compensated effectively.

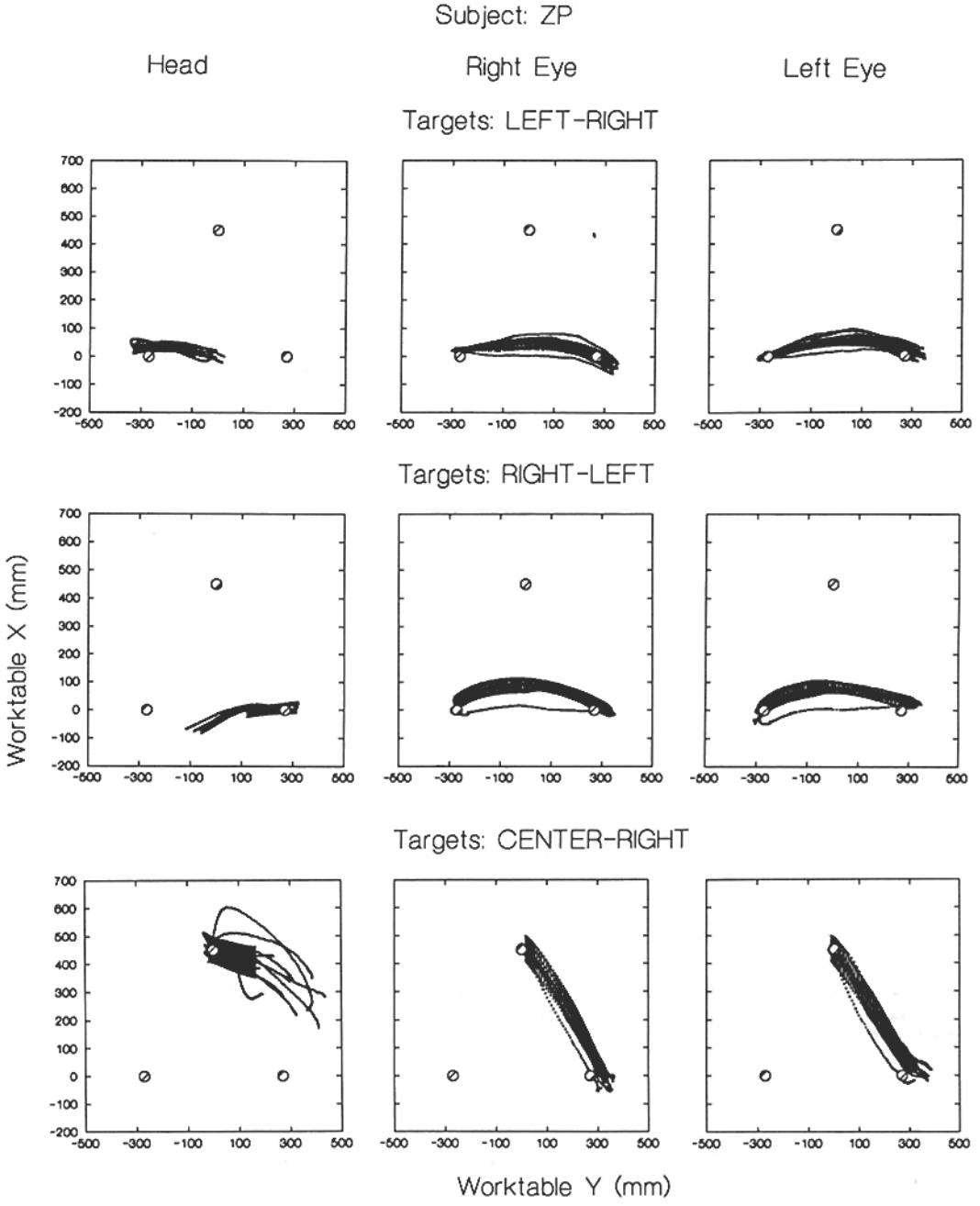

Figure 3. Subject ZP: Two-dimensional trajectories of head (left) and gaze of the right (middle) and left (right) eye superimposed on the Worktable. Thick black bands are from control gaze shifts (mean ± 1 SD); individual thin traces are from push gaze shifts. Open circles denote target positions.

Peak Gaze Velocities

If the VOR were completely effective in compensating for the pushes, then the trajectories of control gaze shifts should be indistinguishable from the trajectories of push gaze shifts (6). This was not the case. Peak right eye gaze velocities, shown in Figure 6, were higher

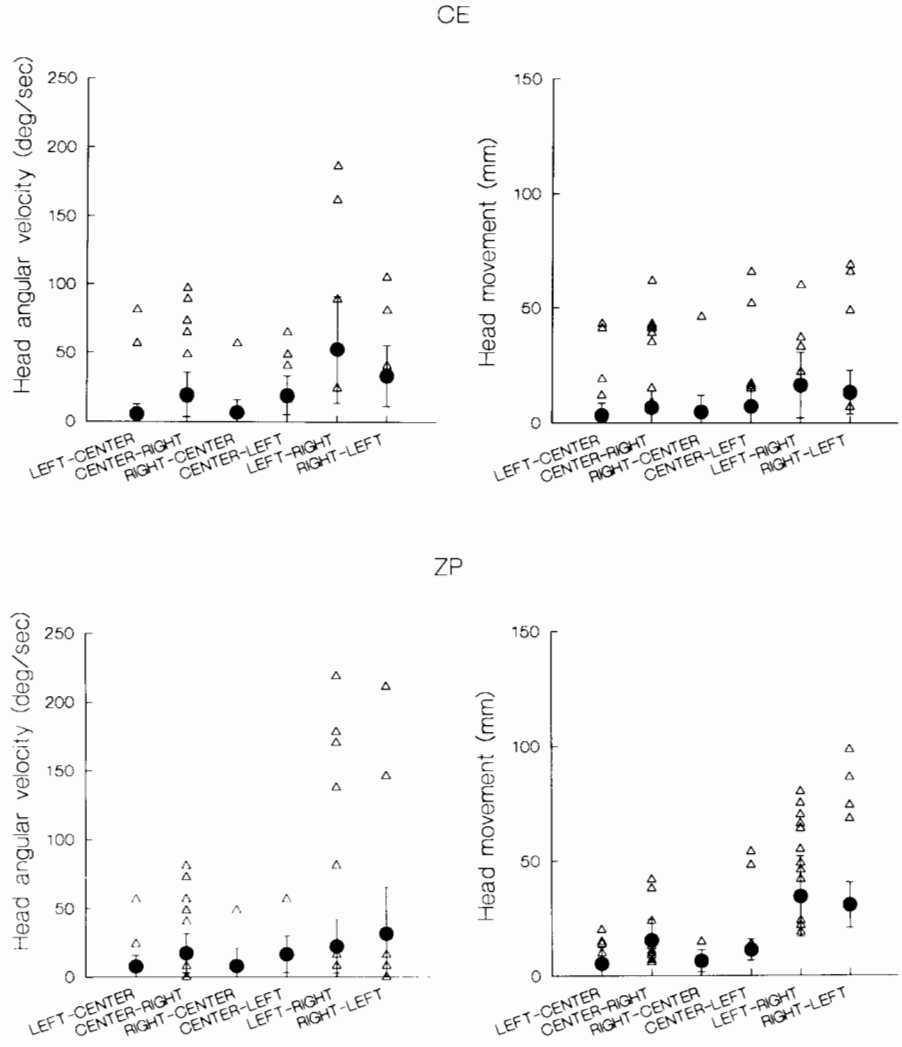

Figure 4. Angular velocity of the head (left) and translational movement of the head (right) for subjects CE (top) and ZP (bottom). Performance in each graph is shown separately for the 6 different gaze shift directions. Filled symbols are from control gaze shifts (mean ± 1 SD), and open triangles are from individual push gaze shifts.

during the push gaze shifts (left eye was similar). In the push gaze shifts, the head was always displaced in the direction of the gaze shift (see Methods), so a higher gaze velocity for these gaze shifts indicates failure of complete compensation by the VOR. Differences between peak velocities of push and control gaze shifts were reliable ($F[1, 869] = 4.2$, $P < 0.05$, for CE; $F[1, 574] = 17$, $P < 0.001$, for ZP). This result shows that the VOR may have contributed to compensation (which it did, as will be shown later), but was not operating at full effectiveness.

Gaze Shift Duration

Others have noted that the VOR is absent, or at least attenuated, during gaze shifts (6–10). In order to explain how gaze shifts can be accurate without a fully effective VOR, models of gaze control have been proposed in which

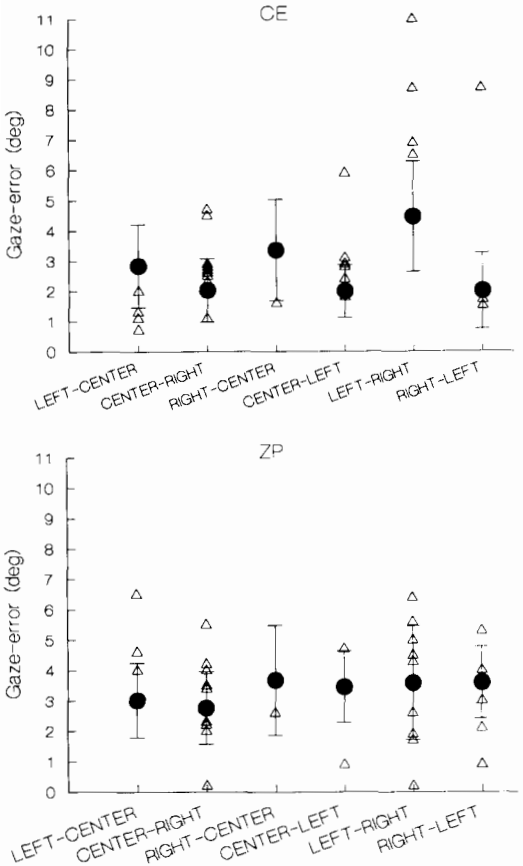

Figure 5. Gaze-error (right eye) for subjects CE (top) and ZP (bottom). Performance in each graph is shown separately for the 6 different gaze shift directions. Filled symbols are from control gaze shifts (mean ± 1 SD) and open triangles are from individual push gaze shifts.

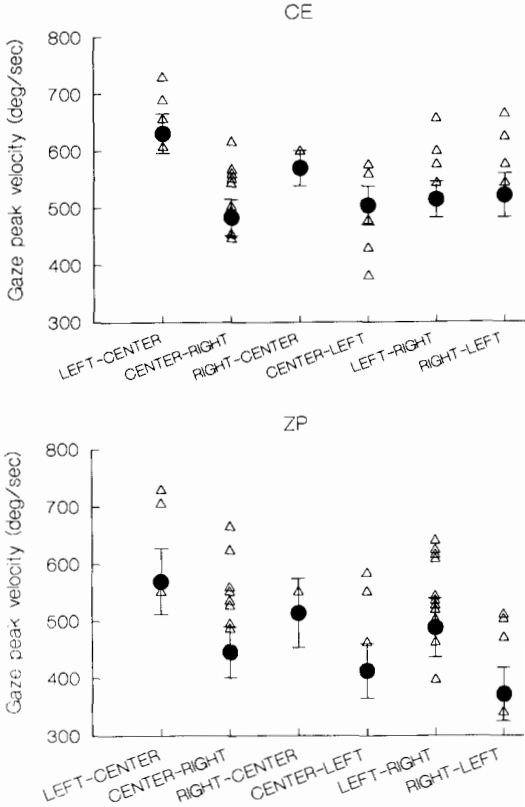

Figure 6. Peak gaze velocity (right eye) for subjects CE (top) and ZP (bottom). Performance in each graph is shown separately for the 6 different gaze shift directions. Filled symbols are from control gaze shifts (mean ± 1 SD) and open triangles are from individual push gaze shifts.

gaze was assumed to continue until gaze error fell below some critical value (see Introduction). At that point, the gaze shift would be terminated. This process would predict that in our experiment, given that the push sent the head in the direction of the gaze shift, durations of gaze shifts should be shorter in push gaze shifts than in control gaze shifts.

Durations of push gaze shifts were shorter than durations of control gaze shifts, as shown in Figure 7. The effect was largest for ZP at the larger target separations (Left-Right or Right-Left). The effect of the push on the duration of gaze shifts was not statistically significant for CE ($F[1, 869] = 2.1$, $P > 0.1$), but was statistically significant for ZP ($F[1, 574] = 14$, $P < 0.001$). As for gaze errors, the interaction between gaze shift type and direction was significant for CE ($F[5, 869] = 3.5$, $P < 0.005$), with the effect of the push on gaze shift duration being greater for larger target separations. The interaction between gaze-shift type and direction was not significant for ZP ($F[5, 574] = 0.75$, $P > 0.5$).

The Contribution of the VOR to Individual Push Gaze Shifts

The results described so far show that there was compensation for the passive displacement of the head, and that the VOR was not

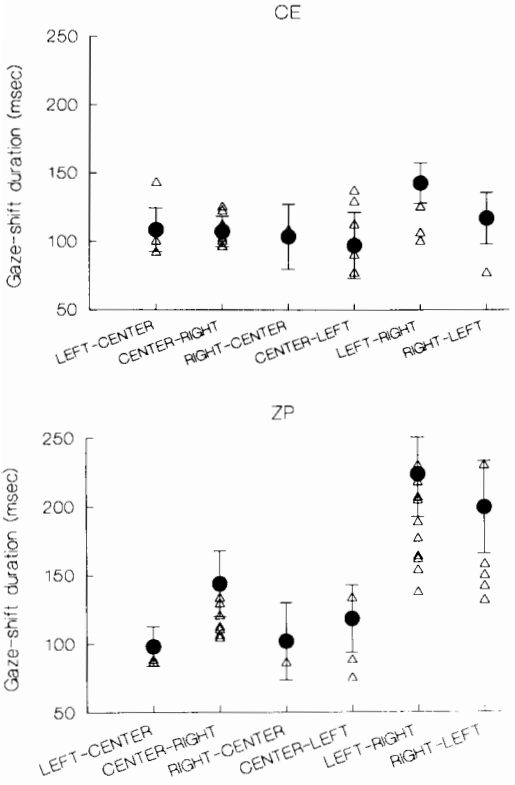

Figure 7. Gaze shift duration (right eye) for subjects CE (top) and ZP (bottom). Performance in each graph is shown separately for the 6 different gaze shift directions. Filled symbols are from control gaze shifts (mean ± 1 SD) and open triangles are from individual push gaze shifts.

fully effective during the gaze shift. Examination of individual gaze shifts shed more light on the role of the VOR. Specifically, (1) the VOR did contribute to the achievement of an accurate gaze shift; (2) the contribution of the VOR varied from one gaze shift to another; and (3) the contribution of the VOR was often different for the horizontal and vertical meridians.

An example of a push gaze shift in which the VOR did *not* make a substantial contribution on the horizontal meridian, but did along the vertical meridian, is shown in Figure 8. This figure shows the eye and head angular position traces of one of subject CE's gaze shifts. The graphs at the bottom show horizontal (left) and vertical (right) head rotations. There are two traces in each head angular position graph. The solid trace, represents mean performance in the control (that is, no push) gaze shifts. The surrounding grey band shows ±1 SD. The dashed line in each head angular position graph shows the head rotation during this gaze shift, in which the subject was pushed. The substantial deviation of this head angular position trace from the controls represents the effect of the push on head rotation.

The remaining graphs in Figure 8 show movements of the right (top graph) and left (middle) eyes. Once again, performance in control gaze shifts (mean ±1 SD) is shown by the solid line surrounded by the gray band, and performance on this gaze shift is shown by the dashed line. First, let us consider the control gaze shifts. Note that in each graph there are two different functions showing performance on the control gaze shifts. One function originates at 0° on the ordinate and then shows a prominent (20°–30°) shift in angular position beginning shortly before time 0 on the abscissa (time 0 was set to the time when eye in head velocity was maximum). This function represents the rotations of the eye in the head (see "Eye-in-head vectors" in the Methods section). The other function from the control gaze shifts begins near an eccentricity of ±30° and then shows a 5°- to 10°-shift in angular position. This function represents the angular position of the target relative to the head. The fluctuations in this target trace were not the result of movements of the target itself (since it was stationary throughout the gaze shift), but instead resulted from movements of the target on the retina caused by both head translation and head rotation (see "Position of the target with respect to the head" in the Methods section). When the mean eye angular position and mean target angular position in the controls coincide, which they do by the end of the gaze shift, then the line of sight has reached the target. (Keep in mind that the solid traces for the control trials represent mean performance, not the individual gaze shifts. Thus, while the mean target and eye angular positions typically coincide by the end of the trial, the target and eye traces for individual gaze shifts would show greater error).

The two dashed lines in each eye angular position graph show eye and target angular

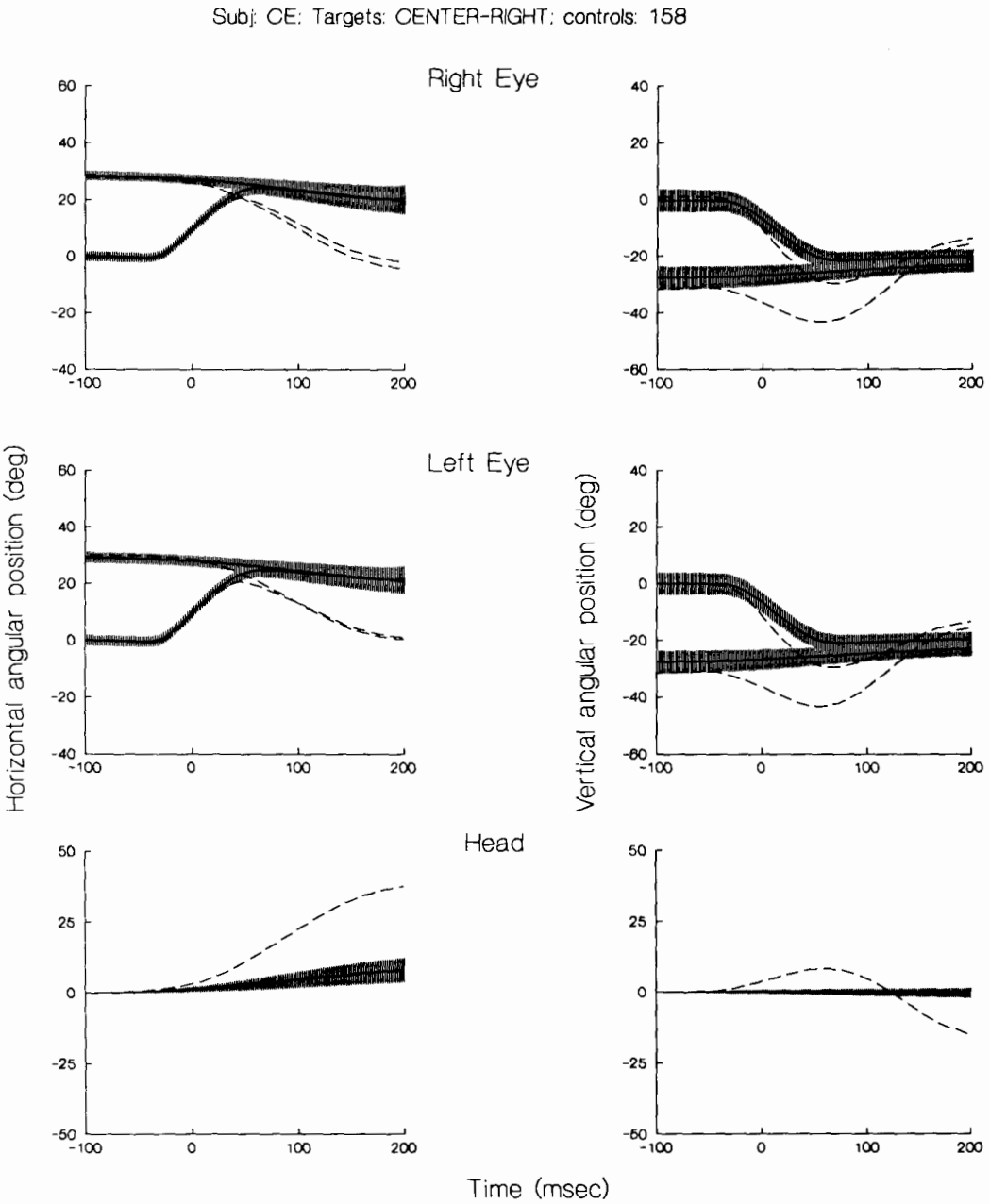

Figure 8. Subject CE's head (bottom), right eye (top), and left eye (middle) angular positions in one gaze shift when shifting gaze between the Center and Right targets. The abscissa shows time; 0 corresponds to the peak velocity of the eye. Horizontal rotations are in the lefthand graphs; vertical rotations in the right hand graphs. In each graph, traces surrounded by gray bands show performance in control gaze shifts, with the central black line showing mean performance and the gray band ±1 SD. The dashed traces in each graph show performance on the current gaze shift in which a push occurred during the gaze shift. Head angular position graphs show head orientation in space. Eye graphs contain two pairs of functions: (1) The pair originating at 0 on the ordinate shows the rotation of the eye in the head relative to the "head axes," described in Methods; (2) The pair originating near +30° or −30° on the ordinate shows the angular position of the target relative to the "head axes." The fluctuations in the target traces are due to movements of the head axes, which were caused by both head rotation and head translations. This example shows compensation late in the gaze shift for the horizontal meridian and early in the gaze shift for the vertical meridian.

position during this gaze shift, which contained a push. The deviation of the *target* trace from the controls shows the effect of the push on target angular position. The deviation of the *eye* angular position trace from the controls shows the way in which rotations of the eye in the head compensated for the effect of the push.

Now consider what happened in the gaze shift shown in Figure 8, looking first at the horizontal movements in the lefthand graphs. The effect of the push on head angular position and on target angular position can be seen near the time peak eye velocity (time 0) was reached. The effect of the push on the angular position of the eye in the head was different. On the horizontal meridian, there was little deviation of this gaze shift's eye angular position trace from the controls until very late in the gaze shift, when the eye had already come quite close to the target. This indicates that compensation for the push, at least on the horizontal meridian, was delayed until late in the gaze shift.

The velocity traces corresponding to these angular position traces are shown in Figure 9. The deviation of this gaze shift's horizontal head velocity trace from the controls (lefthand graphs) shows that the push caused a horizontal head rotation with a peak velocity near 200°/s (Figure 9, bottom). Yet, the horizontal eye-in-head velocity traces show no obvious compensation for the change in head velocity until about 30 msec after peak eye velocity was reached (top and middle graphs). It is not possible to determine, solely from the performance along the horizontal meridian, whether the onset of the compensation was due to the VOR being activated late in the gaze shift or whether it was due to a braking of the eye when gaze error had fallen below some critical value.

Performance on the vertical meridian (righthand graphs in Figures 8 and 9) was less ambiguous. Both the angular position and velocity traces show compensation for the push during the entire course of the gaze shift. Thus, at least along the vertical meridian, the VOR compensated for the head perturbation, and alternative models of gaze control do not appear necessary in this case.

There were cases for CE in which the VOR did compensate for the push early in the gaze shift along the horizontal meridian. Figures 10 (angular position traces) and 11 (velocity traces) show a gaze shift (about 60° in size) with prominent horizontal compensation (this gaze shift was primarily horizontal, with no substantial vertical component). Half of CE's push gaze shifts showed compensation early in the gaze shift on either meridian (similar to Figures 10 and 11), and half showed that compensation was delayed until the line of sight neared the target (similar to Figure 8, horizontal meridian).

Subject ZP's performance was similar to CE's. Figure 12 shows angular position traces for a gaze shift in which horizontal compensation for the push did not occur until late in the gaze shift, when the line of sight was near the target. Figures 13 (angular position traces) and 14 (velocity traces) show an example with compensation early in the gaze shift. ZP showed early compensation on one or both meridians in 39% of his push gaze shifts. Figure 13 also shows another phenomenon that appeared on many gaze shifts. Notice that there was little effect of the push on the vertical head rotations (Figure 13, bottom righthand graphs). On the other hand, the vertical target traces (middle and upper righthand graphs) show substantial effects of the push along the vertical meridian. These differences between the vertical head rotation trace in the bottom graph and the vertical target angular position trace in the upper and middle graphs are due to head translations. The eye angular position traces (Figure 13) and eye velocity traces (Figure 14) both show compensation. Since vertical head rotations were virtually absent, the compensation that occurred must have corrected for the effects of the head translations that affected the vertical target trace.

Discussion

We found effective compensation for passive displacements of the head during shifts of gaze. Our testing conditions were different from those employed in prior investigations of this topic (6–9) and more relevant to the use

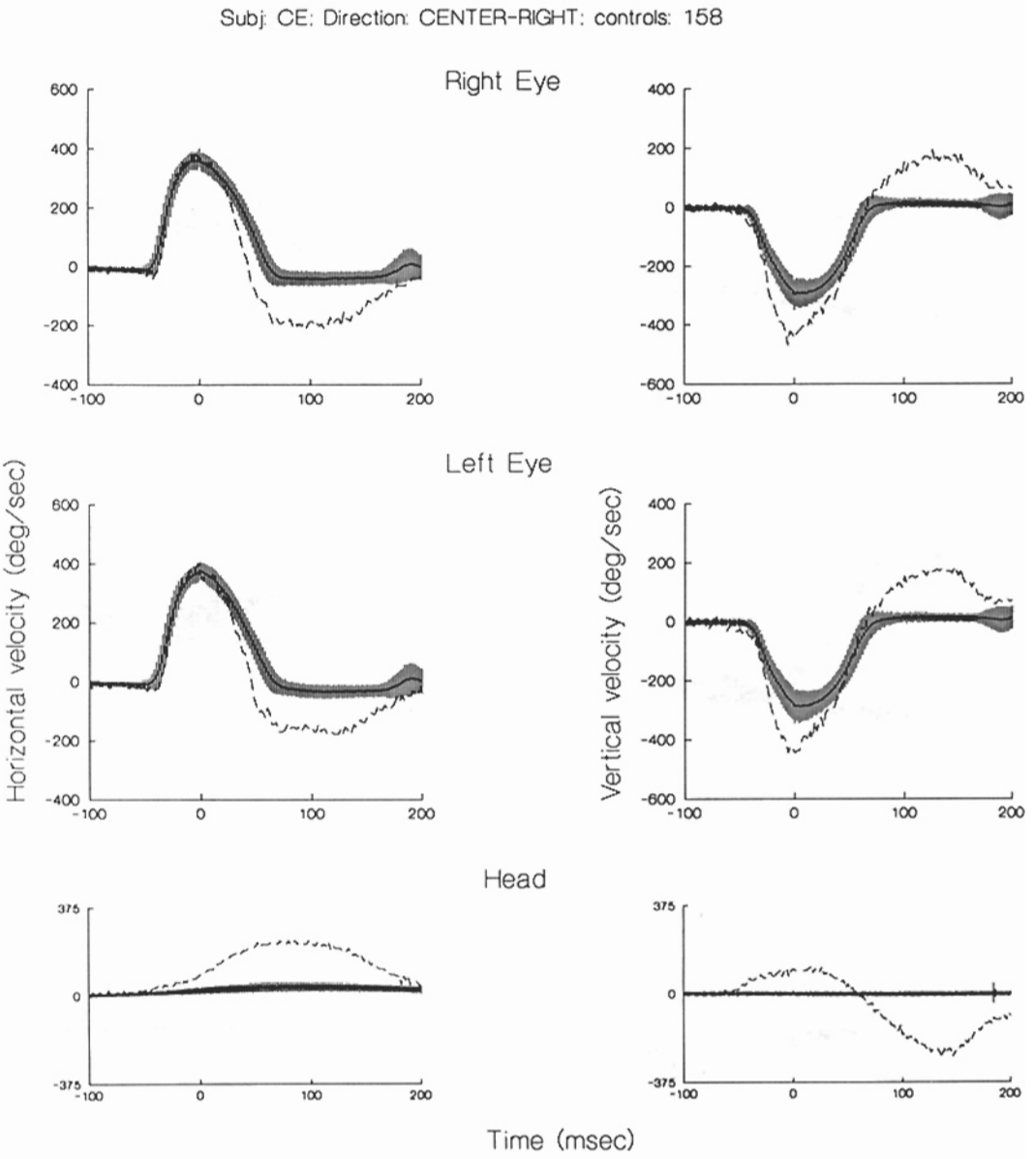

Figure 9. Subject CE's head (bottom), left eye (middle), and right eye (top) velocities when looking between the Center and Right targets. Same gaze shift as shown in Figure 8. The abscissa shows time; 0 corresponds to the peak velocity of the eye. Horizontal velocities are in the lefthand graphs; vertical in the right hand graphs. The trace in each graph surrounded by the gray band shows performance in control gaze shifts, with the central black line showing mean performance and the gray band ±1 SD. The dashed trace shows performance on the current gaze shift in which a push occurred during the gaze shift. Head velocity graphs show head velocity in space. Eye velocity graphs show eye velocity relative to the velocity of the "head axes" described in Methods. This example shows compensation late in the gaze shift for the horizontal meridian and early in the gaze shift for the vertical meridian.

of eye and head movements in everyday life. Targets in the current study were located close to the subject, and the subject was completely unrestrained and free to move the head any way he chose in 3 dimensions. Thus, the high level of compensation demonstrated previously with distant targets and partially restrained heads (6–9) is now shown to apply

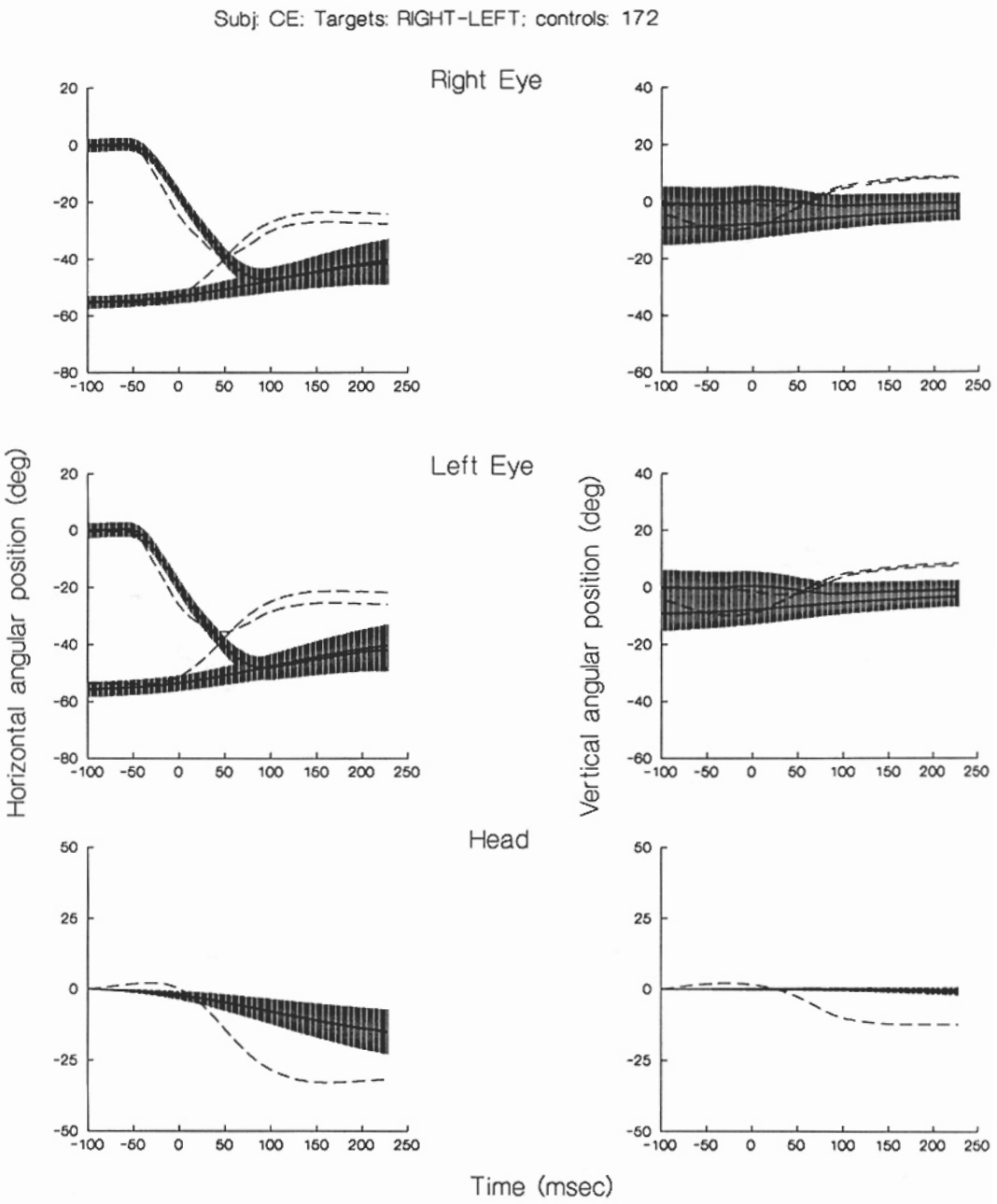

Figure 10. An example of Subject CE shifting gaze between the Right and Left targets. See Figure 8 for significance of the traces. This example shows compensation throughout the gaze shift for the horizontal meridian.

in these more demanding natural viewing conditions.

These results attest to a remarkable ability of the motor system to produce accurate, coordinated movements of head and eye, and to take into account, during the course of the gaze shift, both rotational and translational perturbations to the head. The importance of

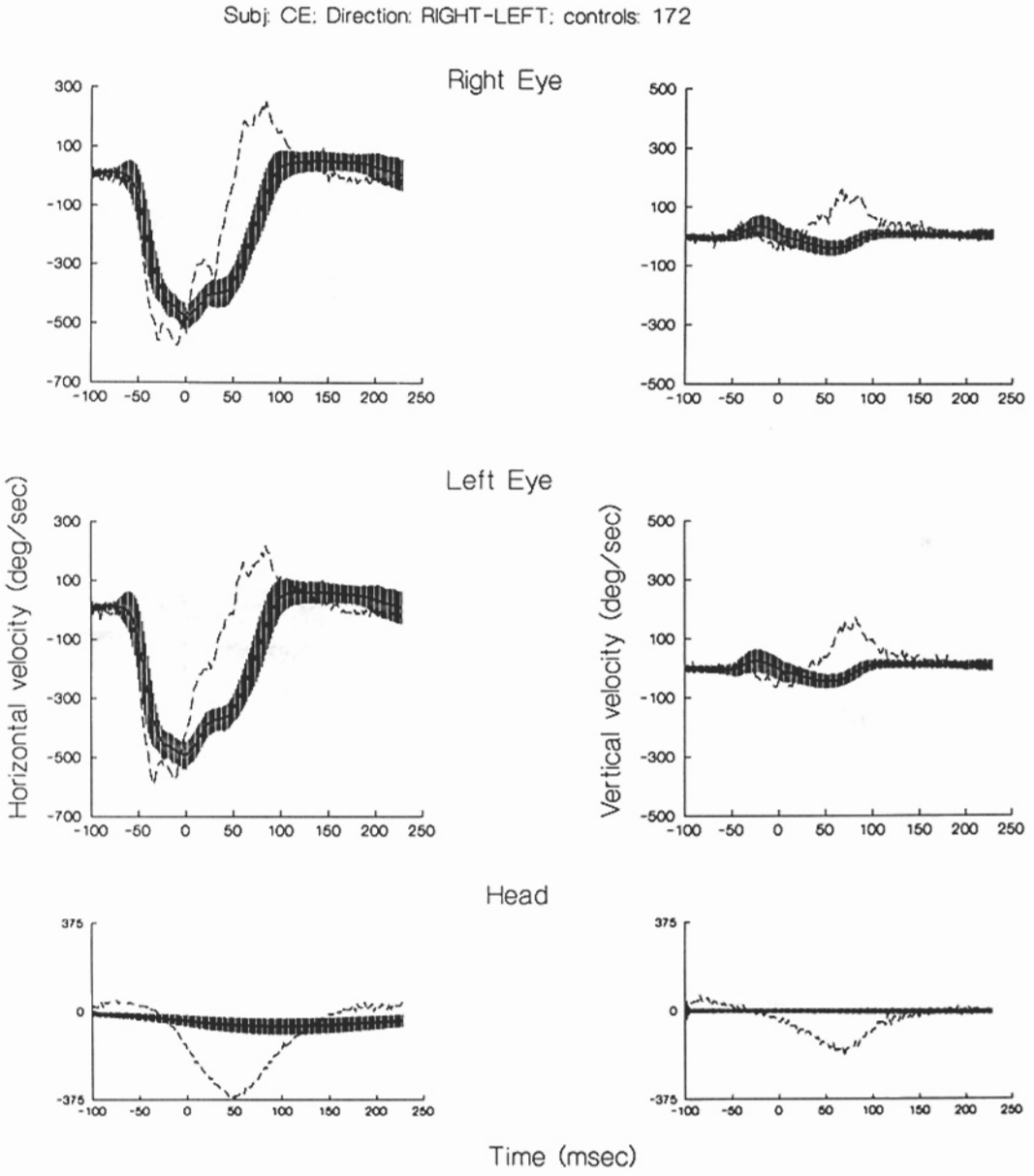

Figure 11. Velocity traces for the same gaze shift as shown in Figure 10. See Figure 9 for the significance of the traces. This example shows compensation throughout the gaze shift for the horizontal meridian.

compensation for passive displacement is that it shows that head–eye coordination is not achieved solely by preprogramming appropriate movements. Head–eye coordination benefits from processes that compensate for head perturbations during the course of the gaze-shift itself.

How is the effective compensation for head perturbations achieved? Previous studies (6–9) rejected the view that compensation is carried out solely by the vestibulo-ocular response. These studies found that the VOR fails to operate, or at least is greatly attenuated, while a gaze shift is in progress (6–10). The size of

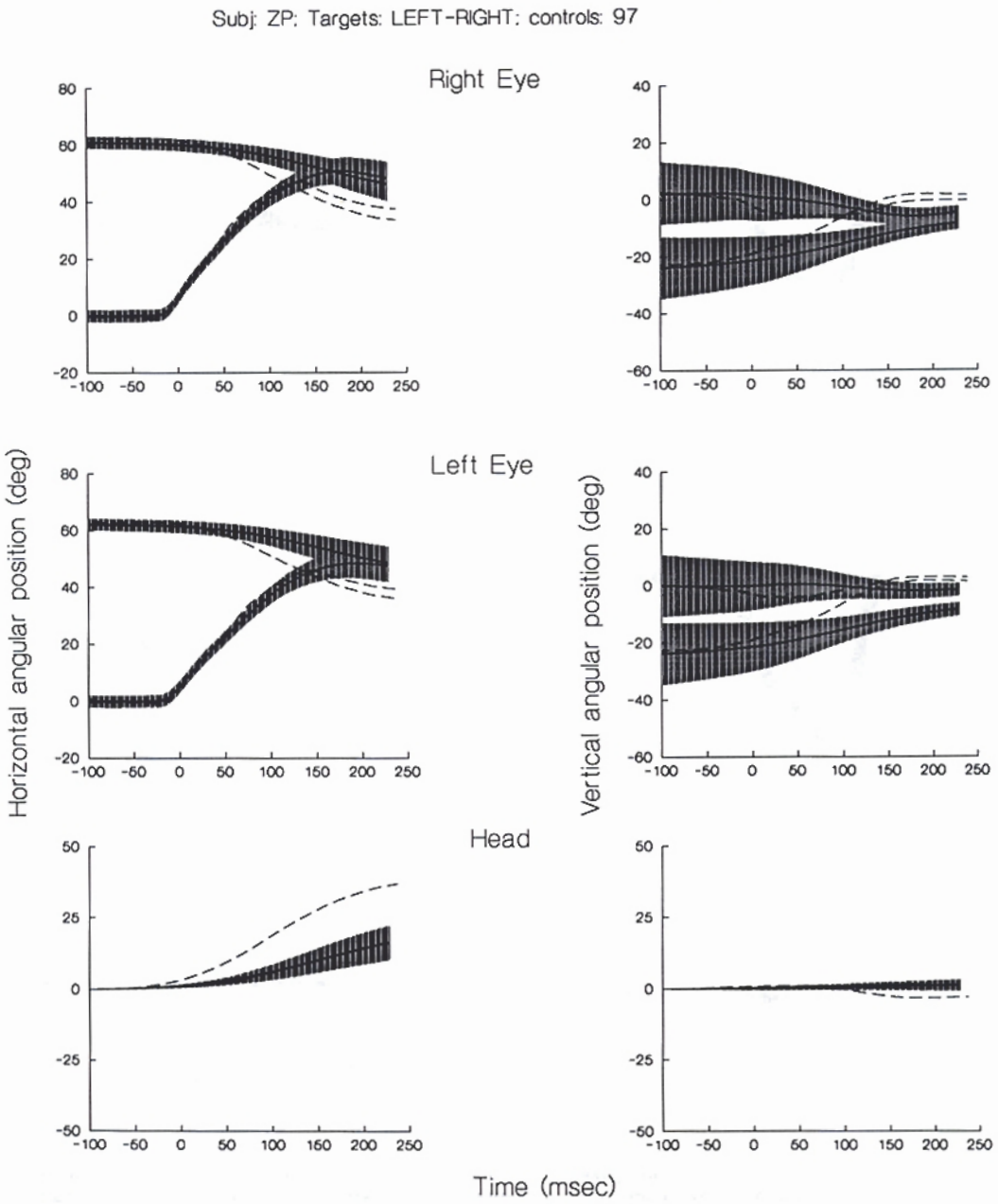

Figure 12. An example of Subject ZP shifting gaze between the Left and Right targets. See Figure 8 for significance of the traces. This example shows compensation late in the gaze shift for the horizontal meridian.

the gaze shifts we studied (30° to 60°) fell in the range where VOR gains of only 0.1 to 0.2 would be expected based on the prior work (6,8,9). In place of the VOR, the prior investigators proposed a different method of gaze control in which gaze error was monitored and a gaze shift terminated once error fell below a criterion value (6–9).

We found, in agreement with these prior reports, many instances in which the VOR ap-

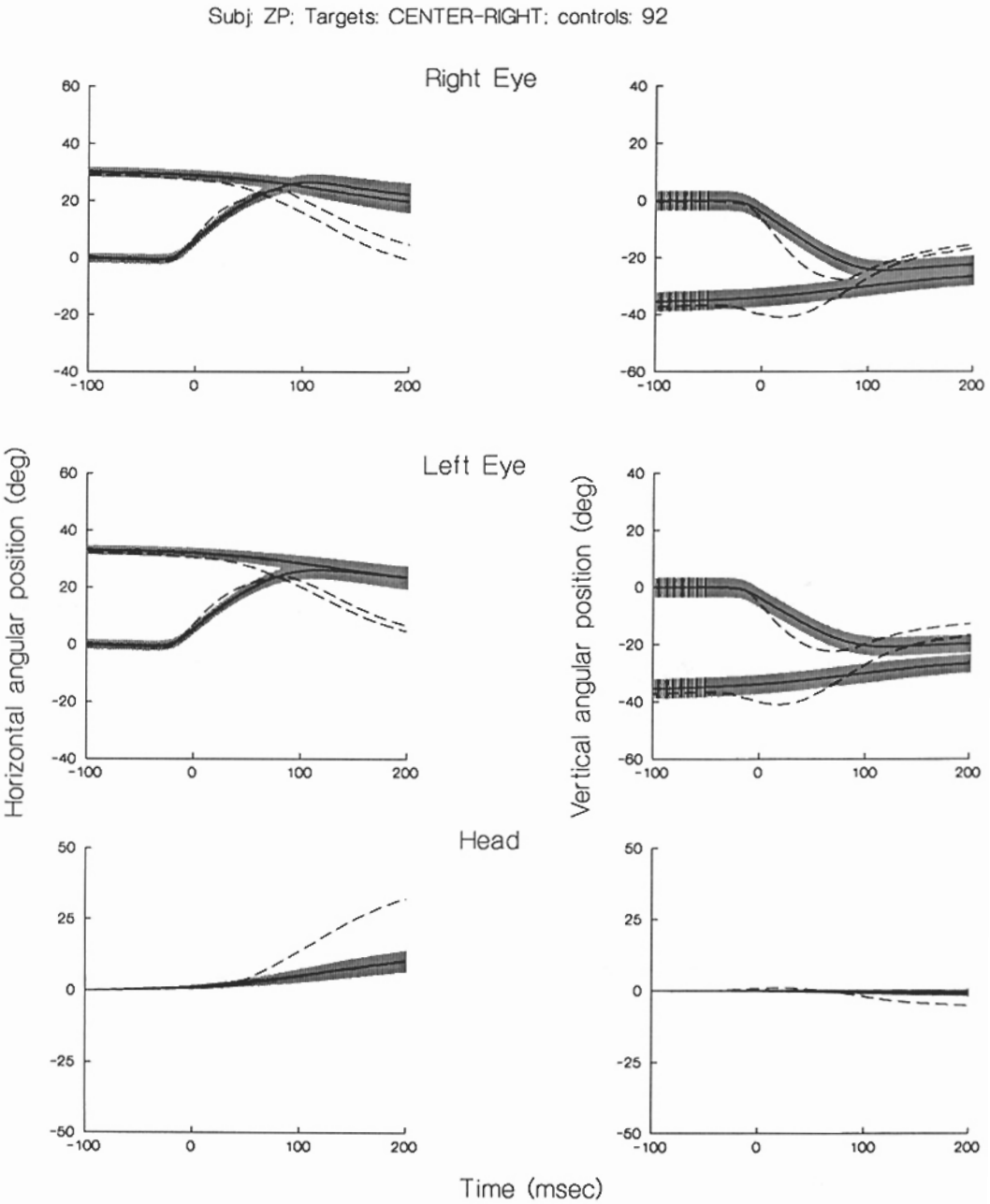

Figure 13. An example of Subject ZP shifting gaze between the Center and the Right targets. See Figure 8 for significance of the traces. This example shows compensation throughout the gaze shift for both meridians.

peared to be inoperative, at least until quite late in the gaze shift, which terminated when the eye was very near to the target. But there were also cases in which the VOR was effective early during gaze shifts on either one or both meridians. We also found examples in which there appeared to be effective compensation for translations of the head, a finding

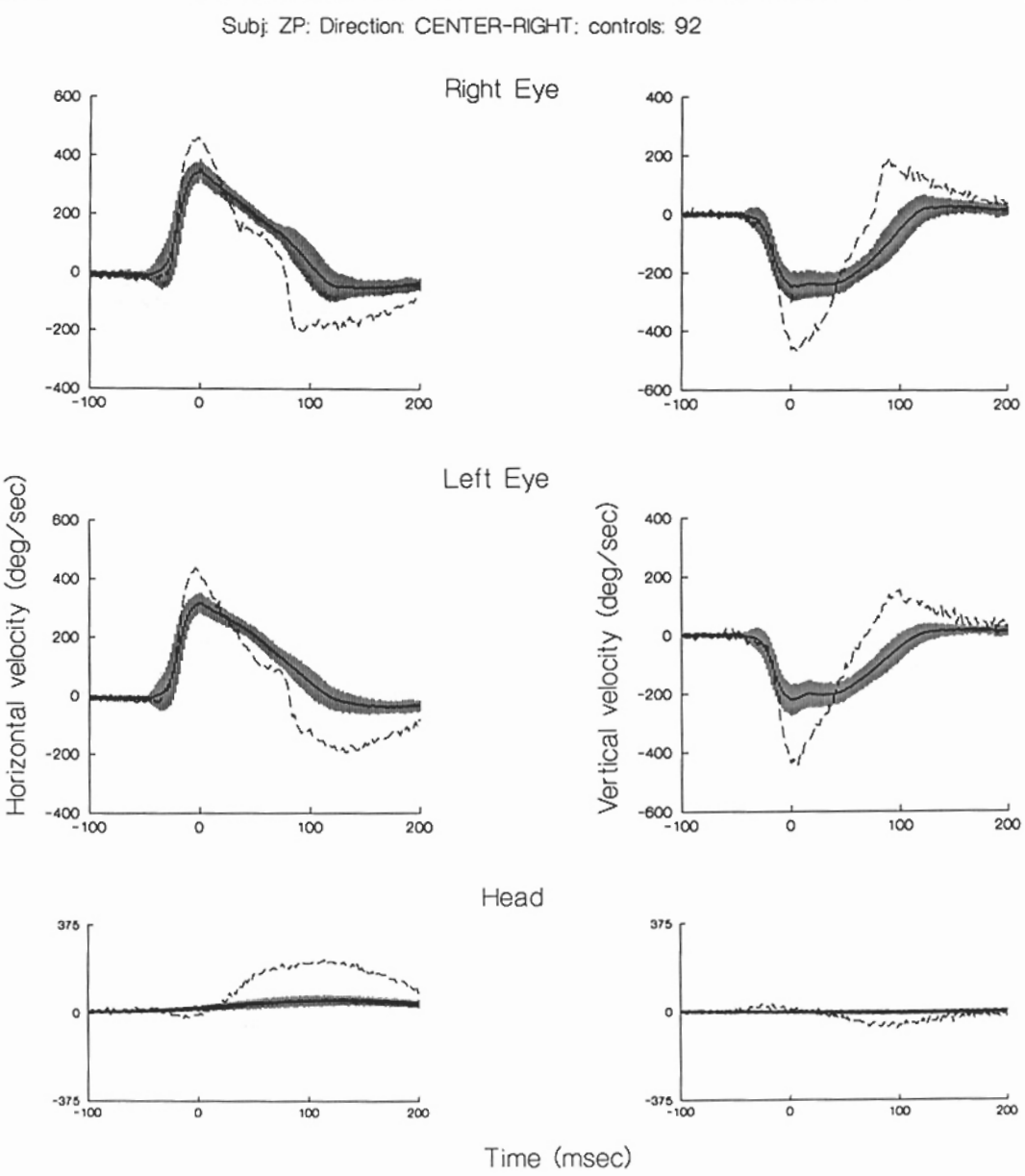

Figure 14. Velocity traces for the same gaze shift as shown in Figure 13. See Figure 9 for significance of the traces. This example shows compensation throughout the gaze shift for both meridians.

that implies that the "linear VOR" (15) can operate during shifts of gaze. Thus, vestibularly based compensatory mechanisms may play a larger role in the control of gaze under natural conditions than would have been expected based on prior work with subjects viewing distant targets with partially restrained heads.

One of the more striking findings was that the contribution of these vestibularly based compensatory systems differed sharply from one trial to the next. From our data there did not appear to be any built-in rule that determined with a high degree of certainty which of these two mechanisms would take the lion's

share of the responsibility for producing accurate gaze.

It is possible that the contribution of the VOR or LVOR to gaze shifts resides under central control. This possibility was raised earlier by Guitton and Volle (7) in an attempt to explain the large individual differences they observed in the contribution of the VOR to gaze shifts. Central control of the contribution of the VOR to gaze shifts seems quite plausible, given the well-known ability of subjects to adjust VOR gain voluntarily during ordinary movements of the head (16,17). VOR gain may be just as susceptible to voluntary or other centrally based modification during a gaze shift.

These speculations about the adjustment of VOR gain during gaze shifts are supported by our recent findings that the velocity of gaze is higher when subjects must tap a sequence of targets than when they simply look at the same sequence (5). In other words, during tapping, VOR gain was reduced in order to bring gaze to the target faster.

Perhaps the best way to account for the characteristics of gaze shifts during head movements is to propose that neither the vestibularly-based compensatory systems, nor alternative mechanisms based on on-line monitoring of gaze position, are, by themselves, adequate to produce accurate gaze shifts under all natural conditions. The key to achieving accurate gaze control may lie in the ability of people to call upon one or the other system at different times and/or to varying degrees (17,18). Evidence for the ability of the human being to juggle the contribution of different subsystems to gaze control seems to be most pronounced when gaze is studied under conditions designed to approximate viewing conditions in the natural world. It may be here that the full extent of the human capacity to produce effective motor control becomes most apparent. From evidence obtained so far, the subsystems that control shifts of gaze function with remarkable effectiveness.

Acknowledgments—This research was supported by grants from the Spatial Orientation program of the Air Force Office of Scientific Research (AFOSR 91-0124; FA-9620-92-J0260; F49620-94-1-0333; and 91-0342). We thank Dr. M. Edwards and M. R. Stepanov for valuable suggestions and technical assistance.

REFERENCES

1. Collewijn H, Steinman RM, Erkelens CJ, Pizlo Z, Van der Steen J. Effect of freeing the head on eye movement characteristics during three-dimensional shifts of gaze and tracking. In: Berthoz A, Vidal PP, Graf W, eds. The head–neck sensory motor system. New York: Oxford; 1992:412–8.
2. Collewijn H, Steinman RM, Erkelens CJ, Pizlo Z, Kowler E, Van der Steen J. Binocular gaze control under free-head conditions. In: Shimazu H, Shinoda Y, eds. Vestibular and brain stem control of eye, head and body movements. Basel: Karger; 1992:203–20.
3. Bizzi E, Kalil RE, Tagliasco V. Eye–head coordination in monkeys: evidence for centrally patterned organization. Science. 1971;173:452–4.
4. Andre-Deshays C, Berthoz A, Revel M. Eye–head coupling in humans; 1: Simultaneous recording of isolated motor units in dorsal neck muscles and horizontal eye movements. Exp Brain Res. 1988: 399–406.
5. Epelboim J, Collewijn H, Edwards M, Erkelens CJ, Kowler E, Pizlo Z, Steinman RM. Coordinated movements of the arm and head increase gaze-shift velocity. Invest Ophthal Vis Sci Suppl. 1994;35:1550.
6. Laurutis VP, Robinson DA. The vestibulo-ocular reflex during human saccadic eye movements. J Physiol. 1986;373:209–33.
7. Guitton D, Volle M. Gaze control in humans: eye-head coordination during orienting movements to targets within and beyond the oculomotor range. J Neurophysiol. 1987;58:427–59.
8. Pelisson D, Prablanc C, Urquizar C. Vestibuloocular reflex inhibition and gaze saccade control characteristics during eye–head orientation in humans. J Neurophysiol. 1988;59:997–1013.
9. Tomlinson RD. Combined eye–head gaze shifts in the primate; 3: Contributions to the accuracy of gaze saccades. J Neurophysiol. 1990;64:1873–91.
10. Tabak S, Smeets JBJ, Collewijn H. Probing the human vestibulo-ocular reflex by high-frequency, helmet-driven head movements. J Physiol. 1994;479: 141P.
11. Epelboim J, Steinman RM, Kowler E, Edwards M, Pizlo Z, Erkelens CJ, Collewijn H. The function of visual search and memory in sequential looking tasks. Vision Res. [In press].
12. Edwards M, Pizlo Z, Erkelens CJ, Collewijn H, Epelboim J, Kowler E, Stepanov MR, Steinman RM. The Maryland revolving-field monitor: theory of instrument and processing its data. Center for Automation Research, University of Maryland at College Park; 1994; CAR-TR-711: 1–129.

13. Collewijn H. Eye and head movements in freely moving rabbits. J Physiol. 1977;266:471–98.
14. Hallett PE. Eye movements. In: Boff KR, Kaufman L, Thomas JP, eds. Handbook of perception and human performance. New York: Wiley; 1986: 10/1–10/112.
15. Paige GD. The influence of target distance on eye movement responses during vertical linear motion. Exp Brain Res. 1989;77:585–93.
16. Barr CC, Shultheis LW, Robinson DA. Voluntary, non-visual control of the human vestibulo-ocular reflex. Acta Otolaryngol. 1976;81:365–75.
17. Collewijn H. The vestibulo-ocular reflex: an outdated concept? In: Allum JH, Hullinger M, eds. Control of posture and locomotion: progress in brain research. Amsterdam: Elsevier; 1989;80:197–209.
18. Steinman RM, Kowler E, Collewijn H. New directions for oculomotor research. Vision Res. 1990;30: 1845–64.